Informatics in Medicine Unlocked 25 (2021) 100698

Contents lists available at ScienceDirect

Informatics in Medicine Unlocked

journal homepage: www.elsevier.com/locate/imu

Genomics and molecular analysis of RPL9 and LIAS in lung cancer: Emerging implications in carcinogenesis

Zodwa Dlamini [a,d,*], Rahaba Marima [a], Rodney Hull [a], Konstantinos N. Syrigos [c], Georgios Lolas [a,c], Lebogang Mphahlele [a], Zukile Mbita [b]

[a] SAMRC Precision Oncology Research Unit (PORU), Pan African Cancer Research Institute (PACRI), University of Pretoria, Hatfield, 0028, South Africa
[b] Department of Biochemistry, Microbiology and Biotechnology, University of Limpopo, Sovenga, 0727, South Africa
[c] 3rd Department of Medicine, National & Kapodistrian University of Athens, Athens, 15772, Greece
[d] Faculty of Health Sciences, School of Clinical Medicine, University of the Witwatersrand, Parktown 2193, South Africa

ARTICLE INFO

Keywords:
Lung cancer
RPL9
LIAS
HSPA9
In silico bioinformatics analysis
qPCR
In situ hybridization

ABSTRACT

Worldwide, lung cancer is a leading cause of cancer-related deaths and is the most commonly diagnosed form of cancer. A major characteristic of lung cancer is its profound clinical, histological and molecular heterogeneity. This heterogeneity is not only spatial but also temporal thus stressing the need for personalized patient-tailored treatment planning. The current optimal treatment planning is currently based on real-time monitoring of the evolving molecular profiling of the tumour throughout the course of the disease and treatment. In the current work, we will investigate the emerging role that that RPL9 and LIAS could have in carcinogenesis. While the aberrant expression of RPL9 has already been shown to occur in colorectal cancer its role in lung cancer is not yet known. In a similar manner, the role of LIAS, as a metabolism-linked gene, in cancer biology and especially in lung cancer is still unknown. Emerging research reveals both RPL9 and LIAS as interacting partners and apoptosis resistance genes. The aim of this study is to determine the differential expression of the *rpl9* and *lias* genes in both normal lung tissue and lung cancer samples. This was achieved by using *in situ* hybridization (ISH) and quantitative Real-time PCR (qPCR). Further data on the role played by RPL9 in lung cancer was established through the use of *in silico* bioinformatic analysis. This was done in order to map biological pathways enriched by the expression of these genes. Both the KEGG pathway and Reactome analysis confirmed the role of these genes in RNA metabolic pathways. Furthermore, RPL9 was shown to play a role in signal transduction, autophagy, and cellular response to stress pathways. The function of these two proteins overlapped with regard to protein metabolism. STRING analysis also demonstrated an interaction between RPL9 and LIAS. Here we propose that the aberrant expression of RPL9 and LIAS may contribute to lung carcinogenesis and can be targeted for molecular therapy.

1. Introduction

Worldwide, Lung cancer continues to be the leading cause of cancer-related deaths in both men and women [1]. A crucial feature of lung cancer is its extreme clinical, histological and molecular heterogeneity. Lung cancer heterogeneity is not only spatial, thus developing between different patients (inter-patient) or different regions within the same tumour (intra-tumour) but also temporal, due to its dynamic evolution with time towards less differentiated, more aggressive and drug-resistant clones. Although multiple factors may contribute to lung cancer, the smoking of tobacco products still remains the leading factor associated with higher incidence of lung cancer as well as higher mortality rates [2]. In developed countries, comprehensive tobacco control programs have led to the decline of lung cancer incidence and mortality rates [3–5]. However, in the developing world, smoking continues to be prevalent in both men and women. Research indicates that lung cancer

Abbreviations: HSPA9, Heat shock 70 kDa protein 9; ICSA1, Iron-sulphur cluster assembly 1; LIAS, Lipoic acid synthetase; LIPT1, Lipoyltransferase 1; LIPT2, Lipoyltransferase 2; NSCLC, non-small cell lung carcinoma; PIK3CA, phosphatidylinositol-4,5-bisphosphate 3-kinase; RP, Ribosomal Protein; RPL6, Ribosomal protein L6; RPL9, Ribosomal protein L9.

* Corresponding author. SAMRC Precision Oncology Research Unit (PORU), Pan African Cancer Research Institute (PACRI), University of Pretoria, Hatfield, 0028, South Africa.
E-mail address: Zodwa.Dlamini@up.ac.za (Z. Dlamini).

https://doi.org/10.1016/j.imu.2021.100698
Received 27 June 2021; Received in revised form 9 August 2021; Accepted 9 August 2021
Available online 11 August 2021

Table 1
Primer sequences for *rpl9* and *lias*.

Rpl9	Forward	CTCCGGGTTGACAAATGGTGG CTCCGGGTTGACAAATGGTGG
Rpl9	Reverse	CCCATTCTCCTGGATAACAACG CCCATTCTCCTGGATAACAACG
Lias	Forward	TAAGACTGCAAGAAATCCTCCTCC TAAGACTGCAAGAAATCCTCCTCC
Lias	Reverse	CACAAGGATTTTTGGATTCCTTTCC CACAAGGATTTTTGGATTCCTTTCC
Gopdh	Forward	TGCACCACCAACTGCTTAGC TGCACCACCAACTGCTTAGC
Gapdh	Reverse	GGCATGGACTGTGGTCATGAG GGCATGGACTGTGGTCATGAG

mortality rates in these countries is higher, despite lower incidence rates. This may be due to multiple factors including environmental contaminants. In addition to this, social and cultural barriers combined with inadequate access to health facilities can lead to diagnosis at later stages of the disease and poorer treatment outcomes. These delays in diagnosis and treatment have a serious impact on the overall survival rate [6]. The prognosis of lung cancer is generally grim, with 5-year survival rate is approximately 15,7% [1]. Adenocarcinoma, a non-small cell lung carcinoma (NSCLC) type, is the most common histologic subtype of lung cancer in both men and women, followed by squamous cell carcinoma, large-cell carcinoma, and small-cell lung carcinoma [7,8]. Currently pathologic stage is the most important system to predict survival in patients with NSCLC and to define groups with similar treatment strategies. However, the discovery of molecular markers such as EGFR, ALK, KRAS, HER2, MET, BRAF, PIK3CA, MEK1, NRAS, AKT1 and ROS1 that have been identified in NSCLC [9–12] could be used as potential therapeutic targets that are more effective and with fewer side effects than current treatments. There is a significant necessity to increase the knowledge of the genetic factors that play a role in lung cancer susceptibility and as such molecular gene profiling promises to yield potential diagnostic, prognostic, and therapeutic targets leading to improved diagnosis and treatment of lung cancer.

This is the case with Ribosomal protein L9 (RPL9) is a component of the 60S rRNA subunit for protein synthesis. Baik et al. [13] correlated the aberrant expression of RPL9 with the Id-1/NF-κB signalling pathway and cell survival in colorectal cancer. In addition, Zhang et al. [14] suggested that the upregulated human RPL9 expression appears to be involved in uncontrolled growth by promoting stress-mediated survival in colorectal cancer. Eid et al. [15] concluded that *rpl9* is an anti-apoptotic gene encoding a Ribosomal Protein (RP) in yeast. Furthermore, various ribosomal proteins (RPs) have been found to be overexpressed in different cancer cells and are also associated with the development and progression of malignant cancers [16]. Besides protein biosynthesis, additional ribosomal function(s) of RPL9 are not fully understood, particularly in lung cancer. *Rpl9* has different splice variants and Lezzerini et al., 2020 showed that *Rpl9* variants can differentially impair ribosome function and cellular metabolism. For instance, variants that retain the 5' UTR stabilize p53 thus impairing growth and differentiation of erythroid cells. Bioinformatics analysis performed in the current study highlighted a probable link between RPL9 and the protein Lipoic acid synthetase (LIAS). Both RPL9 and LIAS have been reported as apoptotic resistance genes [17]. A genome wide study of methylation profiles in ovarian cancer performed by Ref. [18] revealed both *lias* and *rpl9* were hypomethylated in cancer tissue when compared to normal tissue. Methylation changes are frequently found in cancers, and the loss of DNA methylation, also known as hypomethylation may play a role in tumorigenesis [19,18]. In this study, our main aim was to measure the expression levels of RPL9 and LIAS in lung cancer compared to normal lung tissue and to determine, using bioinformatics analysis, if the differential gene expression patterns of *rpl9* and *lias* may play a role in apoptotic and cell survival pathways in lung cancer.

2. Materials and methods

2.1. In silico bioinformatics

Bioinformatics tools were used to map the biological and molecular pathways enriched by RPL9 and LIAS. The Reactome database (https://reactome.org/) version 72 was used to map the biological pathways involving both RPL9 and LIAS. The GenBank accession number of *rpl9* (NM_000661) and *lias* (NM_006859) were uploaded. The human identifiers and IntAct interactors functions were selected to increase the analysis background. To investigate the protein-protein interactions involving RPL9 (NM000661) and LIAS (NM_006859), the STRING database was employed [20]. KEGG pathway analysis by DAVID v6.8 [21] was used to visualise the enriched pathways. Based on initial results obtained using *in silico* analysis the protein Lipoic acid synthetase (LIAS) was identified as a novel probable downstream effector of RPL9 activity. This led to the bioinformatics analyses being performed using LIAS as an additional query.

In order to further analyse the predicted protein interactions identified using STRING, it was necessary to construct 3D homology models for proteins in the RPL9 interaction network, including LIAS, ICSA1, HSPA9, RPL6 and RPL9. This was done using the SWISS-model [22]. Further validation of the predicted models and an assessment of their quality were done by comparing them to their templates using the ProSA web server, this provided z value scores for the individual models. Docking analysis between proteins that were indicated as interacting as per the STRING analysis was performed using ClusPro 2.0 [23]. As such docking analysis was performed between the 3D homology model of LIAS and that of ISCA1 and RPL9, as well as between the 3D homology model of HSPA9 and that of ISCA1 and RPL6. Following ClusPro analysis, the Protein interaction calculator bioinformatics tool was used to identify bonds that formed between these interacting proteins within a 6 Å (A) cut off. In addition to this, the models were further analysed using the USCF Chimera tool [24]. As a result of these bioinformatics analyses, the expression pattern of LIAS was also determined in conjunction with that of RPL9 in normal lung tissue, multiple forms of lung cancer tissue and cell lines derived from healthy lung tissue and lung adenocarcinoma tissue.

2.2. Sample collection

Normal control and lung cancer tissues were acquired from the National Health Laboratory Services (NHLS), Department of Pathology, Johannesburg, South Africa with written informed patient consent. The tissues were handled as stipulated in the Ethical clearance as per the guidelines and regulations approved by the Human Research Ethics Committee of the University of the Witwatersrand (Clearance Number: M050308). These tissue samples were diagnosed and classified as normal tissue or subtypes of lung carcinoma by a Consultant Pathologist (from the School of public health, University of the Witwatersrand). Cancer cases provided were adenocarcinoma (NSCLC), large cell carcinoma, squamous cell carcinoma and small cell carcinoma.

2.3. Cell culture

Two cell lines were also used in this study, a primary fibroblast lung cell line, MRC-5, and lung adenocarcinoma cell line, A549. The MRC-5 (ATCC CCL171) and A549 (ATCC CCL185) cell lines were obtained from the American Type Culture Collection (ATCC). Both cell lines were grown in Dulbecco's Modified Eagle Medium (DMEM) (Life Technologies) supplemented with 10% heat-inactivated foetal bovine serum (FBS) (Sigma-Aldrich) and 1% penicillin and streptomycin. Cells were cultured at 37°C in a humidified incubator with 5% CO_2. Cells were cultured for 2–3 days to reach ~70% confluency prior to trypsinization for subsequent experimental purposes.

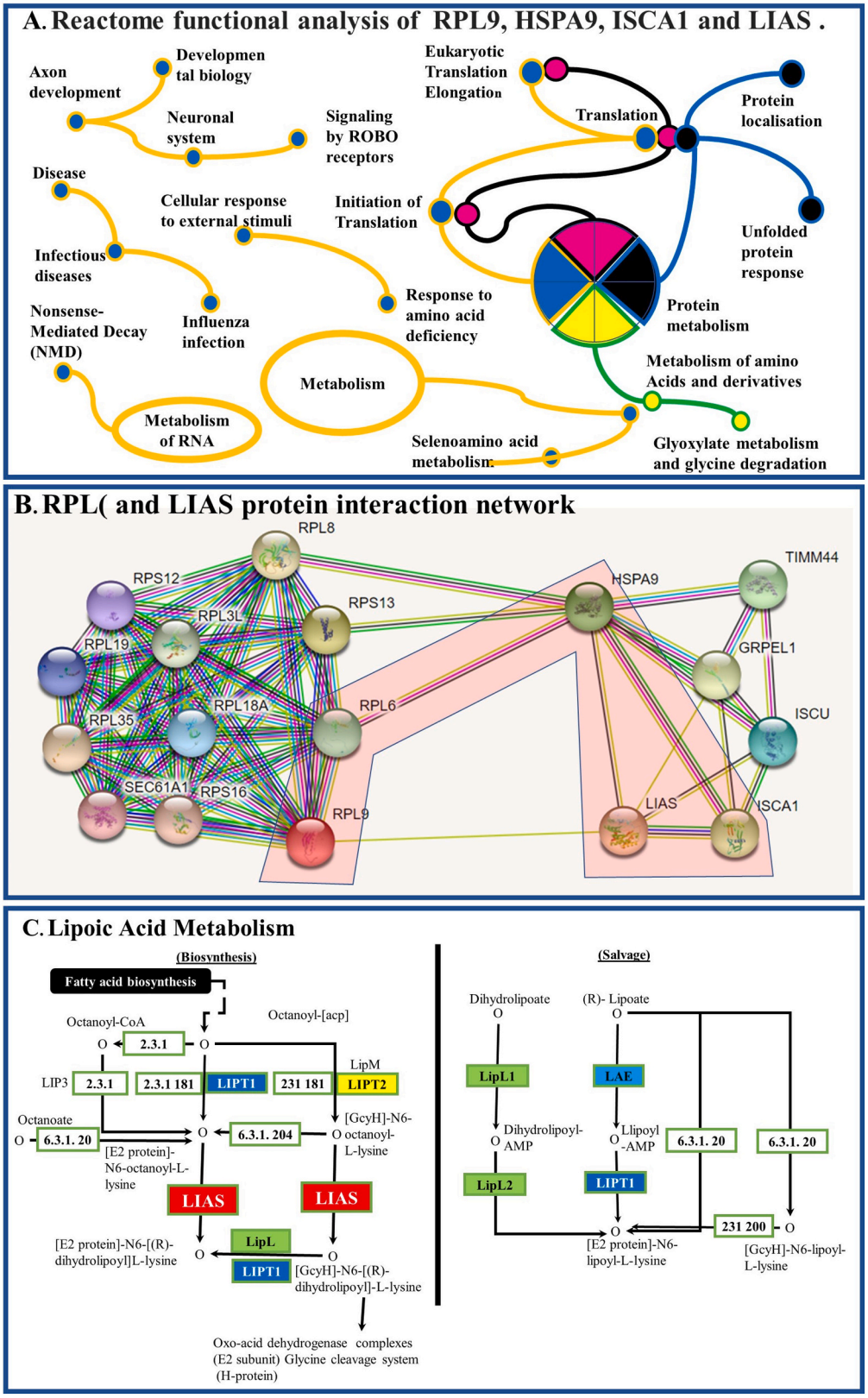

Fig. 1. Reactome, STRING and KEGG pathway analyses. **(A)** Represents a genome wide map analysis of RPL9, HSPA9, ISCA1 and LIAS genes using the Reactome pathway database. The orange lines with blue circles represent the pathways involving RPL9. The purple circles with black lines represent the pathways involving ISCA1. The yellow circles with green lines represent the pathways involving LIAS. The black circle with blue lines, represent the pathways involving HSPA9. HSPA9 was shown to be involved in virtually all areas of the pathway but these were omitted from the figure for clarity. These proteins are all involved in protein metabolism **(B)** Shows the STRING analysis of both RPL9 and LIAS, showing the interaction between the ribosomal proteins and HSPA9 and the interaction between this protein and ISCA1 and LIAS. It also shows a weak interaction between RPL9 and LIAS. **(C)** represents KEGG pathway analysis LIAS showing its role in Lipoic acid metabolism. (For interpretation of the references to color in this figure legend, the reader is referred to the Web version of this article.)

Table 2
Details for homology models constructed for proteins identified by STRING analysis.

Protein	Template	Structure ref	Seq Identity	Seq Similarity	GMQE	QMEAN	Z Score
RPL6	CryoEM structure of human ribosome	[29]	100.00	0.61	0.63	3.68	−3.29
HSPA9	X-ray crystal structure of DnaK	[30]	61.94	0.48	0.70	0.92	−11.63
ISCA1	X-ray crystal structure of ICSA (mercury derivative)	[31]	38.1	0.81	0.42	−2.87	−5.29
LIAS	X-ray crystal structure of lipotehoic acid synthetase	[32]	45.00	0.42	0.55	−1.12	−9.3

2.4. In situ hybridization calorimetric and fluorescent detection

In order to synthesize RNA probes for the localization of *rpl9* and *lias* transcripts, primers were designed to amplify cDNA fragments from their mRNA transcripts. The resulting amplicons were cloned into the pGEM-T Easy vector (Promega, USA), and sequenced at Inqaba Biotec, South Africa and confirmed using the NCBI BLAST search tool. DIG-labelled anti-sense and sense RNA probes were then generated using T7 or Sp6 polymerase (Roche Diagnostics, Germany). *In situ* hybridization was performed on 4 μm tissue sections prepared from paraffin wax blocks of tissue from normal and lung cancer tissues. Hybridization was performed overnight at 55 °C followed by washing sections with 2 × saline sodium citrate (SSC) buffer and 1 × SSC at 55 °C. Sections were then washed in 0.5 × SSC and 0.1 × SSC at room temperature and blocked in 10% (w/v) blocking reagent (Roche Diagnostics, Germany).

The colorimetric detection was performed by incubating hybridised sections in *anti*-Digoxygenin (DIG) alkaline phosphatase-conjugated antibody solution (Roche diagnostics) for 1hr at room temperature. Bound probe antibody complexes were then visualised using 5-bromo-4-chloro-indolyl phosphate/nitro blue tetrazolium (Roche diagnostics) counterstained with Mayer's Haematoxylin (Sigma). Stained sections were then mounted with aqueous mounting medium (Serotec).

Two strategies (colorimetric and flourimetric) were used for the localization of rpl9 and *lias* mRNA in lung cancer and noncancerous tissues. To detect the *lias* mRNA localization using *in situ* hybridization, the DIG-labelled probe was utilized and stained with Anti-DIG-conjugated alkaline phosphatase. The localised probe was then detected utilizing the substrate NBT/BCIP, which produces a purple/blue precipitate depending on the hydrolysis of BCIP and reduction of NBT (colorimetric). A second strategy employed an anti-DIG conjugated fluorescein isothiocyanate (FITC) antibody using Fluorescence *in Situ* Hybridization (FISH) as previously reported [25]. The sections were incubated in anti-DIG conjugated to FITC (Roche Diagnostics). The stained sections were then mounted using SlowFade Light Antifade Kit (Molecular Probes).The localised probe was detected using fluorescence microscopy, utilizing the Axio software (Zeiss, Germany) for taking images.

2.5. Real time-quantitative PCR (RT-qPCR)

Quantitative Real-time PCR reactions were done using the FastStart DNA Master SYBR Green I kit (Roche Diagnostics, Germany). Gene specific primers (Table 1) for rpl9 [NM_000661], *LIAS* [NM_006859]. were designed using the primer 3 tool (http://primer3.wi.mit.edu/). GAPDH [NM_002046.5] was used as an internal control.

Gene specific expression PCR was performed using 1 μg of cDNA and 0.016 ρmol/μl of each gene specific primer. PCR-grade H_2O was used in place of template to serve as a no template control. The change in gene expression level between test (cancer) and control (normal) samples was expressed as fold change using the Livak and Schittman method [26] as per the formula below:

$$\text{Fold change} = 2\text{-}[\Delta CT\ (\text{test}) - \Delta CT\ (\text{calibrator})]$$

2.5.1. Statistics analysis

The data from three independent experiments for both FISH (the fluorescence intensities) and real-time qPCR were presented as mean ± standard error of mean (SEM) and analysed using GraphPad Prism version 5. The significance differences among the groups were considered at $p \leq 0.05$ using ANOVA, utilizing Tukey's Post Hoc Test.

3. Results

3.1. RPL9 pathway mapping and protein interaction analysis identified LIAS as a protein of interest

The Reactome database identified that RPL9 is involved in protein metabolism and translation as well as playing a role in autophagy, immune response, signal transduction and the cellular response to external stimuli (Fig. 1A). The overexpression of RPL9 in cancers is thought to allow for increased protein expression in cancer cells [27]. Reactome and STRING analyses of RPL9 identified that most proteins that interact with RPL9 are other ribosomal proteins. However, by searching for proteins that interact with these other ribosomal proteins, apart from other ribosomal proteins, revealed other proteins of interest. The Reactome analysis of these proteins revealed that they also play a role in protein metabolism (Fig. 1A). Of particular interest was the identification of the heat shock protein, HSP9A. Not only do heat shock proteins play roles in protein expression and metabolism, but they also play a role in stress responses. One of the proteins that interact with HSP9A that STRING identified is the Iron-sulphur cluster assembly 1 (ICSA1) homolog, which in turn interacts with Lipoic acid synthetase (LIAS) (Fig. 1B).

When the Reactome database was used to analyse the functions of LIAS, ISCA1 and HPSA9 it showed an overlap with the function of RPL9 in the role of protein metabolism. However, unlike RPL9, LIAS is not involved in translation, but it is involved in amino acid metabolism. The proteins linking RPL9 and LIAS such as HSPA9 and ISCA1 also show functions in protein and amino acid metabolism. RPL9 interacts with other ribosomal proteins RPL6 and RPS13 and these interact with the stress protein HSPA9. HSPA9 is a chaperone that assists in protein folding and interacts with both RPL6 and RPL8. Both these proteins are components of the ribosome and interact with RPL9. Both ISCA1 and HSPA9 are involved in translation, but the heat shock protein is involved in protein transport and the misfolded protein response. ISCA1 is involved in protein maturation through post-translational modification (Fig. 1A). ISCA1 in particular is involved in the iron-Sulphur cluster scaffold assembly pathway. This pathway provides stability during the folding of proteins [28]. In addition to ICSA1, LIAS interacts strongly with proteins involved in metabolism such as Lipoyltransferase 1 (LIPT1) and Lipoyltransferase 2 (LIPT2).

STRING analysis showed a weak interaction between LIAS and RPL9. KEGG analysis showed that LIAS is involved in lipoic acid metabolism (Fig. 1C). The lipoic acid cofactor plays an essential role in the activity of the multi-enzymatic complexes of the mitochondrial energy metabolism is revealed here (Fig. 1C). As a result of these analyses the expression of LIAS in lung cancer tissue and cells was determined in conjunction with RPL9 expression.

3.2. Homology modelling and docking analysis

The 3D structures of human RPL9, RPL6, HSPA9, ISCA1 and LIAS were constructed using the 3D structural models of homologous proteins

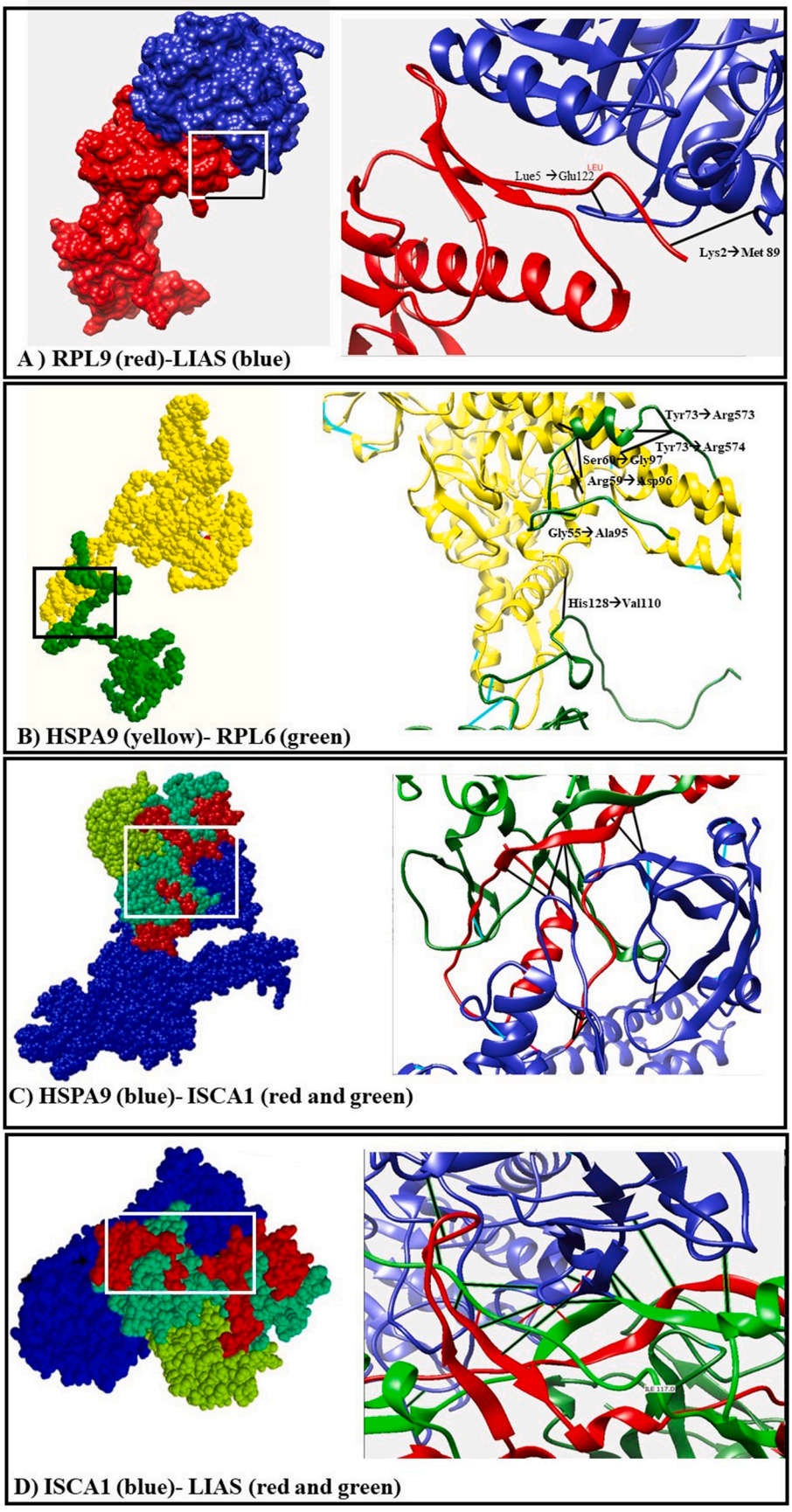

Fig. 2. Protein Interaction Calculator and Chimera analysis of ClusPro interaction models: The ClusPro analysis resulted in the construction of multiple docking models. The RPL9-LIAS model (A) was only predicted to have two H bonds within the 5 Å cu off range. The STRING analysis predicted only a weak interaction between these two proteins, and this docking analysis seems to validate this prediction. The STRING analysis predicted a stronger interaction between RPL6 and HSPA9 (B) and this is reflected by the increase in the number of H bonds predicted in the docking model. Analysis of the docking models for HSPA9-ISCA3 (C) and ICSA1-LIAS (D) predicted multiple H bonds between these proteins. Both these models show bonds including hydrogen bonds, ionic bonds, and hydrophobic bonds. The multiple colours in the interacting reflect different regions of the protein. For HSPA9-ISCA1, the most bonds were present between the unstructured C terminal of ISCA1 (chain B) and the C terminal alpha helices of HSPA-9. For LIAS9-ISCA1, the most bonds were present between the unstructured central region of ISCA1 and the central alpha helices and beta sheet of LIAS (chain B and D). (For interpretation of the references to color in this figure legend, the reader is referred to the Web version of this article.)

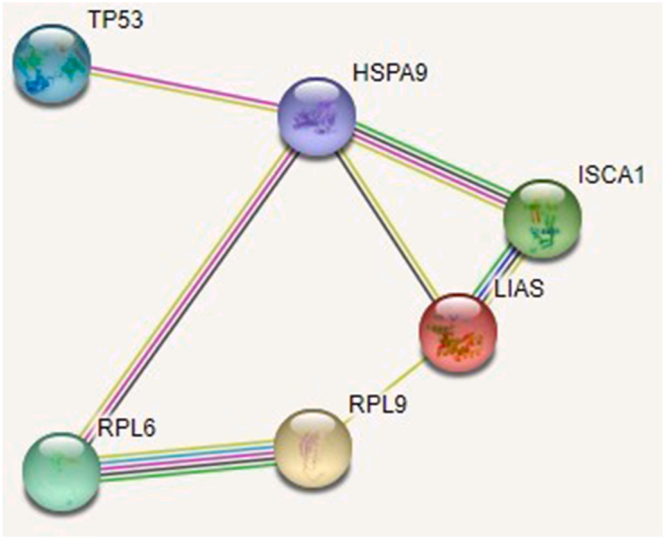

Fig. 3. STRING protein-protein interaction pathway analysis showing interactions between TP53 and the proteins of interest in this study. STRING analysis of the interactions of all the proteins in the identified interaction pathway between RPL9and LIAS showed that the HSPA9 heat shock protein linking LIAS and RPL9 interacts with p53, where it acts as a negative regulator of p53.s function.

as specified in Table 2. The resulting models are presented in Supplementary Fig. 2. The PDB entries of these templates as well as the sequence identity and homology values, compared to the target proteins, are given in Table 2. These models were assessed for their quality and stereochemical quality. The Prosa server was used to analyse the models and the Z scores are also given in Table 2. All these scores are negative, indicating that the residue energies together with pair energy, combined energy, and surface energy were all negative and had comparable surface energy affinities with their template structures.

Ramachandran plots of these various models revealed that the majority of the amino acids in all models are in a ψ distribution consistent with a right-handed α-helix and are therefore likely to be good quality and reliable models (Supplementary Fig. S1). Altogether, no abnormalities were observed in the validation process. Docking analysis between the 3D homology models was performed based on the protein-protein interactions predicted by STRING, using ClusPro. The details of the docking models constructed in this way are given in Supplementary Table 1. All docking analyses resulted in 27–29 models for each interaction. The models for graphic representation and further analysis were selected based on multiple factors. Those that were selected had the highest member numbers, had the most energetically favourable central model as well as the model with the lowest energy. The selected models were model 01 for RPL9-LIAS docking, model 02 for HSPA9-RPL6 docking, model 03 for LIAS-ISCA1 docking and model 01 for HSPA9-ISCA1 docking.

The protein interaction calculator bioinformatics software [33] as well as the UCSF Chimera software was used to analyse predicted bond formation between proteins in the ClusPro models. Analysis of the RPL9-LIAS models showed that only two Hydrogen bonds were formed within 5 Å (Fig. 2A). This matches the STRING prediction that this would be a very weak interaction. There were more hydrogen bonds formed in the HSPA9 – RPL6 interaction model (Fig. 2B), but both the HSPA9-ISCA1 (Fig. 2C) and ISCA1-LIAS (Fig. 2D) interaction models have a large number of predicted Hydrogen bonds. The HSPA9-ISCA1 model has predicted interactions between all three chains of ISCA1 and HSPA9. These include multiple hydrophobic interactions, ionic interactions, and hydrogen bonds. These bonds all formed within 5 Å. The same is true of the PIC analysis of ISCA1-LIAS ClusPro models (Fig. 2D).

Bioinformatics analysis was also carried out in order to establish if any of these proteins interact with tumour suppressor TP53. This was done to shed light the roles of RPL9 and LIAS in pro-or-*anti*- cell survival mechanisms. As expected only the heat shock protein HSPA9 interacts with p53 (Fig. 3). This interaction was confirmed with the IntAct tool. This confirmed that this interaction has been determined experimentally. Here it was shown that HSPA9 sequesters p53 in the cytoplasm preventing it from performing its tumour suppressor function [34]. The lack of interaction of either RPL9 or LIAS with TP53 is not surprising as their role in cell proliferation and cell death is not yet or has only been partially established.

3.3. Elevated expression of lias and rpl9 in human lung cancer

In Situ hybridization showed elevated transcription levels of *rpl9* and *lias* in lung cancer compared to normal tissue. The mRNA levels of *rpl9* and *lias* transcripts, established through staining intensity, were compared between normal and lung cancer tissues. Additionally, the transcripts were localised to different cell types within the tissue samples based on the staining patterns observed. The sense probe was used as the negative control. Based on colorimetric and fluorescent analysis, it was observed that both genes were transcribed in normal and cancerous tissues, but the mRNA levels of both genes were higher in cancer tissues. Based on the analysis of the fluorescence intensity observed in the FISH staining results as shown in Fig. 4, the transcription levels of both *rpl9* and *lias* were significantly upregulated (**$p < 0.01$) in small cell lung carcinoma and lung adenocarcinoma (*$p < 0.05$). However, there was no significant increase in the transcription levels of either gene observed in squamous cell lung carcinoma ($p > 0.05$). These results indicate that transcription levels of *rpl9* and *lias* are (Fig. 4) highest in small cell lung carcinoma, followed by adenocarcinoma and is the lowest in squamous cell lung carcinoma. The overall transcript levels of *rpl9* is high relative to that of *lias* in normal lung tissue and lung cancer. This may imply the unelucidated significant role of RPL9 in lung cancer. These findings are in correlation with those of [13] where elevated levels of RPL9 were seen in colorectal cancer.

ISH also showed more accumulation of *rpl9* in lung cancer compared to the normal tissues (Fig. 5). *Rpl9* mRNA was localised to the type I pneumocytes, lymphocytes and Macrophages in squamous cell lung carcinoma. It was also detected in columnar ciliated cells of the bronchial gland. In the small Cell Lung Carcinoma, *rpl9* was detected in tumour cells that resemble lymphocytes. *Lias* mRNA is detected in the columnar epithelial cells of lung adenocarcinoma (Fig. 5).

3.4. RT-qPCR reveals elevated transcription levels of rpl9 and lias in lung cancer

Quantitative real-time PCR demonstrated increased levels of rpl9 and lias mRNA in lung adenocarcinoma cancer. Using the $2^{-[\Delta CT\ (test) - \Delta CT\ (calibrator)]}$ method [26], fold changes representing change in *rpl9* and *lias* gene expression between test (cancer) and control (normal) were calculated. *LIAS* was found to be 4-fold up-regulated in lung adenocarcinoma while *rpl9* was found to be 8-fold up-regulated. Fig. 6 illustrates upregulated gene expression levels of *lias* and *rpl9* in lung cancer cells (A549) versus in normal lung fibroblasts (MRC-5). Both *rpl9* and *lias* were shown to be expressed at elevated levels in lung cancer.

4. Discussion

In silico bioinformatics studies were performed to identify proteins that interact with RPL9 and may play a role in the development and progression of lung cancer. The STRING analysis initially only identified ribosomal proteins as interacting proteins. However, the extension of the examination of the interactions using these other ribosomal proteins identified the HSPA9 heat shock protein. This protein was selected as Intact and STRING analysis identified that this protein interacts with p53. Further downstream analysis in STRING using RPL9, RPL6, one of

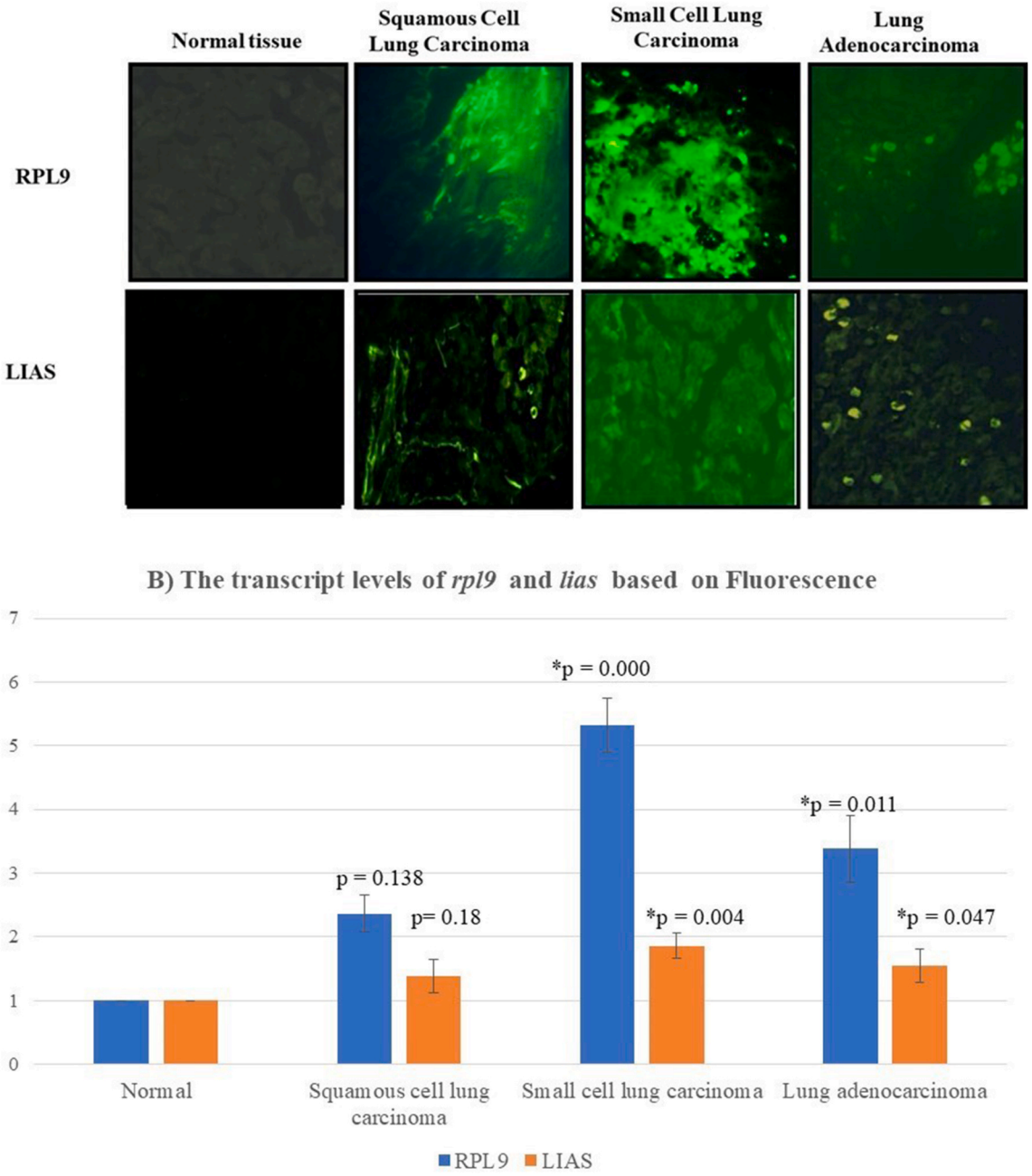

Fig. 4. Detection of transcript level of RPL9 and LIAS using Fluorescent in situ hybridization (FISH). (A) Fluorescent staining of *Rpl9* and *Lias* mRNA in normal lung tissue as well as various types of lung cancer, including squamous cell lung carcinoma, small cell lung carcinoma and adenocarcinoma (400 × Magnification). (B) The intensity of the fluorescent signal was used as an indication of the transcript levels in each of the samples was determined and then this was translated to a staining intensity score relative to the normal tissue. Both *rpl9* and *lias* transcription was shown to be highest in small cell lung carcinoma. The transcription levels of both *rpl9* and *lias* increased in all cancer types when compared to normal lung tissue. Transcription of both genes was significantly higher in lung adenocarcinoma and small cell lung cancer. The presence of the transcripts in different cell types within the tissues was also established.

the proteins joining RPL9 and HSPA9 in the interaction network, and HSPA9 as query proteins, identified multiple interactors. The use of the Reactome pathway analysis tool to search for proteins with an overall similar function identified ISCA1 and LIAS to confirm that these proteins all play a role in protein and amino acid metabolism. A weak interaction was also identified between RPL9 and LIAS and this in conjunction with their shared interacting network, identified LIAS as an important novel target for research into the role that RPL9 may play in lung cancer. Based on this bioinformatics analysis, the gene expression of LIAS was analysed in conjunction with that of RPL9.

Further analysis of these protein interactions was performed by constructing 3D homology models of these proteins. These models were analysed for their quality, and it was shown that these were good quality models. ClusPro and PIC analysis indicated that there were very reliable solid predictions for strong interactions between HSPA9 and ISCA1 and between ISCA1 and LIAS. However, the docking models did not show any strong reliable docling model for the interaction between RPL9 and LIAS. This was not surprising considering the weak interaction predicted by the STRING analysis. ClusPro analysis did predict a more reliable docking model for the interaction between RPL6 (a known interactor with RPL9) and HSPA9. However, bond prediction between the two proteins in the docking model using UCSF Chimera, revealed the

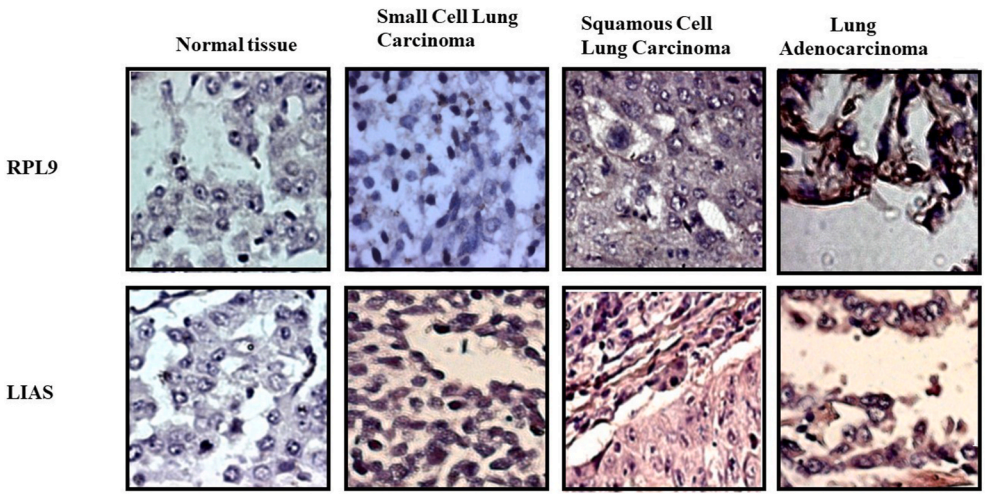

Fig. 5. Localization of *rpl9* and *lias* in lung cancer tissue and normal lung tissue by ISH. BCIP staining and Mayer's Haematoxylin counterstaining was used to stain localise an assess the transcription of *rpl9* and *lias* in various lung cancer tissues as well as in normal lung tissue. The staining for *rpl9* was strongest in the squamous cell lung carcinoma and adenocarcinoma. The staining for *lias* was equally intense across all three types of lung cancer. In both cases higher levels of *rpl9* and *lias* were detected in lung cancer tissue compared to normal lung tissue. The staining also allowed the transcripts to be detected at higher levels in certain cell types within the tissues. For instance, *rpl9* was detected in type I pneumocytes, the macrophages and the lymphocytes of squamous cell lung carcinoma, in cells resembling lymphocytes in small cell lung carcinoma and in the columnar ciliated cells of the bronchial gland in lung adenocarcinoma. *Lias* mRNA was detected in the lymphocytes of small cell lung carcinoma and in the columnar epithelial cells.(400 × Magnification).

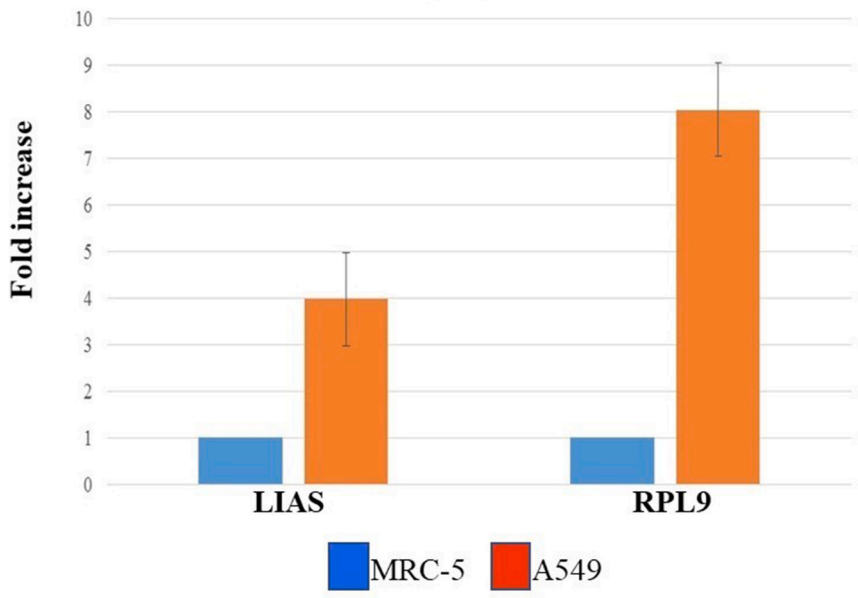

Fig. 6. RPL9 and LIAS gene expression level by RT-qPCR in lung cells. Both RPL9 and LIAS genes show an upregulated expression in the adenocarcinoma cancer cells relative to primary normal fibroblast MRC-5 cells.

presence of at least six H bonds within the 5 Å range. The presence of electrostatic interactions was also indicated (data not shown). Once again, this confirms the intermediate strength interaction predicted through STRING analysis.

In situ hybridization showed localization of *rpl9* and *lias* in both normal and cancerous lung tissue sections. The intensity of localization of these two gene targets, particularly *rpl9* was greater in cancer than in normal tissue. The mRNA levels of *rpl8* were greater in small cell lung carcinoma, followed by adenocarcinoma, and then squamous cell lung carcinoma. *Lias* mRNA was also present in the cytoplasm and literature indicates that LIAS is expressed in the mitochondrion [1,2,4,5,35] and RPL9 localises in the cytoplasm as a ribosomal protein [13]. Co-localization studies will be interesting to determine and confirm the co-localization of RPL9 and LIAS. However, the transcript level of *lias* was the highest in small cell carcinoma, followed by adenocarcinoma and squamous cell carcinoma. Overall, the transcript levels of *rpl9* were high relative to that of *lias*. Quantitative real time PCR confirmed an increase in transcription of *rpl9*and *lias* in lung cancer relative to its normal counterpart. It is also confirmed that *rpl9* mRNA levels are higher than those of *lias*. This may be linked to the vital function performed by RPL9.

It is already known that HSPA9 plays a role in downregulating the tumour suppression activity of p53. The correlation between aberrant LIAS expression levels and the upregulated glycine biosynthetic pathway in rapidly proliferating cells has also been reported [2] and this higher expression is associated with high breast cancer mortality rates [36]. LIAS produces lipoic acid which is an essential cofactor that is required for the activity of five multi-enzymatic complexes. These five complexes include four 2-oxiacid dehydrogenases; namely, pyruvate dehydrogenase (PDH), branched-chain ketoacid dehydrogenase (BCKDH), 2-ketoglutarate dehydrogenase (2-KGDH) and 2-oxoadipate dehydrogenase (2-OADH). These complexes play a significant role in

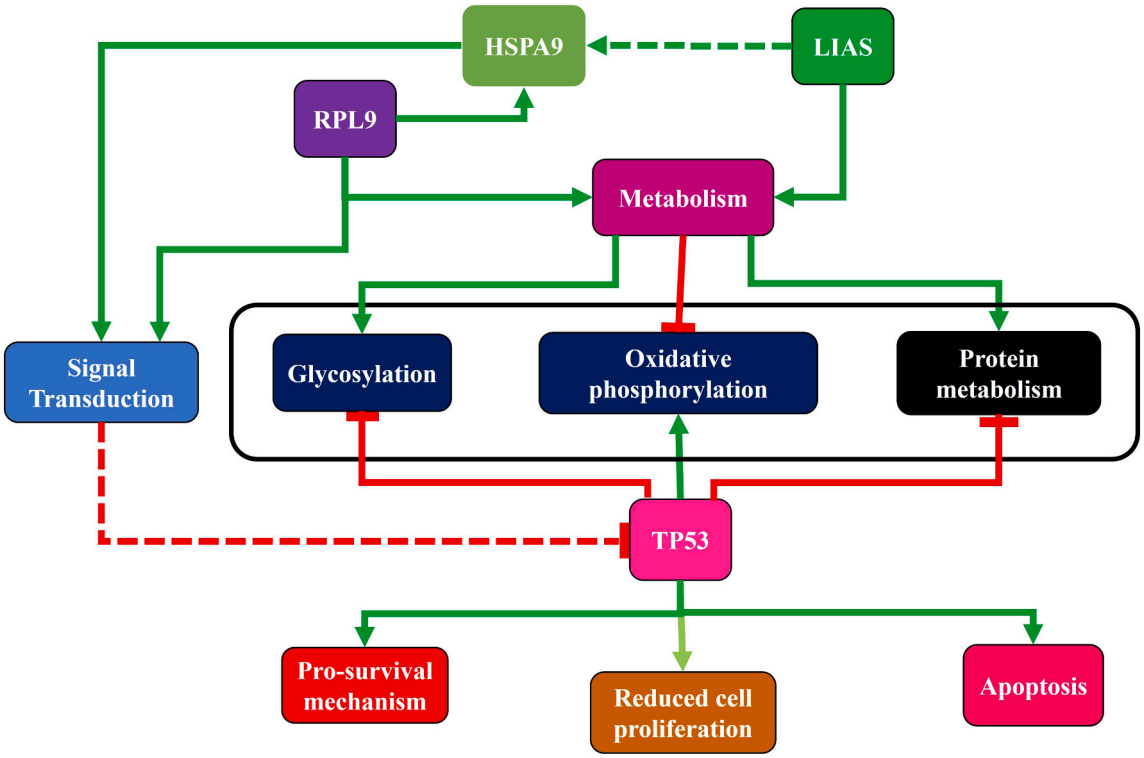

Fig. 7. The summary of RPL9 and LIAS roles in lung cancer. Increased gene expression of RPL9 and LIAS may promote metabolism, cell survival and cell proliferation. Through the transcriptional regulatory role of p53, these pro-survival mechanisms may be repressed, thus leading to reduced cell proliferation and or cell death. RPL9 and LIAS may also promote metabolic pathways such as glycolosis by inhibiting p53, which acts to increase oxidative phosphorylation.

the mitochondrial energy metabolism [37]. The fifth complex is the 2-oxoacid dehydrogenase complex. Additionally, the glycine cleavage system (GCS) also plays an important role in mitochondrial energy metabolism [38]. Metabolic reprograming, shown by the increased nutrient uptake and utilisation, has been proposed to be a hallmark of cancer [36,39,40]. While various studies have revealed both *rpl9* and *lias* act as apoptosis resistance genes and are hypomethylated in cancer, it is not surprising that genes and their products that may be involved in similar biological and pathophysiological pathways and may interact together. Wang et al. (2018) identified both *RPL9* and p53 in a PPI network of proteins that play a role in venous thromboembolism (VTE). Notably, the upregulation of the expression of both these genes in lung cancer warrants further investigation, particularly through the nuclear factor signalling pathway and glycine biosynthesis pathway. This investigation may be persuaded as potential biomarker and therapeutic targets in lung cancer.

5. Conclusion

Abnormally proliferating cells such as cancer cells prefer excessive glucose uptake and less oxidative phosphorylation, a situation known as the Warburg effect [41]. For rapid proliferation and consistent cell survival, cancer cells need to reprogram the metabolic pathways, particularly those relating to macromolecules including lipids and proteins. RPL9 and LIAS, play a significant role in protein and lipid metabolism. Although several studies such as Wang et al. (2018) reveal the potential interaction of RPL9 and p53 using bioinformatics approaches in vascular disease, the lack of experimentally and validated results for the p53-RPL9/LIAS interaction warrants further investigation. Here, we propose that altered signal transduction pathways which favour cell survival and a reduced overall oxidative state in cells, is potentially induced by the aberrant expression of RPL9 and LIAS. The altered expression of these proteins may favour uncontrolled cell proliferation in lung cancer. Furthermore, both RPL9 and LIAS seem to play a pro-survival or anti-apoptotic role in lung cancer. These results, further corroborate the importance of these proteins in cancer progression through their predicted interactions with p53 as it can be seen in Fig. 7.

Declaration of competing interest

The authors declare that they have no known competing financial interests or personal relationships that could have appeared to influence the work reported in this paper.

Acknowledgements

We would like to thank the National Health Laboratory Service (NHLS), Wits Department of Pathology for providing the tissue sections.

Appendix A. Supplementary data

Supplementary data to this article can be found online at https://doi.org/10.1016/j.imu.2021.100698.

Funding

The South African Medical Research Council (SAMRC) and the National Research Foundation (NRF) funded this project.

Author contributions

Zodwa Dlamini-conceptualization, funding acquisition, writing, review and editing. Rahaba Marima-formal analysis, writing, review and editing. Rodney Hull-formal analysis, writing, review and editing. Konstantinos Syrigos – formal analysis, writing, review and editing. Georgios Lolas - formal analysis, writing, review and editing. Lebogang Mphahlele - formal analysis, writing, review and editing. Zukile Mbita-formal analysis, writing, review and editing.

Consent

The authors declare there is no conflict of interest and no images require consent for use.

References

[1] Fitzmaurice C, et al. The global burden of cancer 2013. JAMA Oncol 2015;1:505–27.
[2] Barta JA, et al. Global epidemiology of lung cancer. Ann Glob Health 2019;85.
[3] Jemal A, et al. Global cancer statistics. CA Canc J Clin 2011;61:69–90.
[4] Thun MJ, et al. 50-year trends in smoking-related mortality in the United States. N Engl J Med 2013;368:351–64.
[5] Youlden DR, et al. The International Epidemiology of Lung Cancer: geographical distribution and secular trends. J Thorac Oncol 2008;3:819–31.
[6] Goss PE, et al. Challenges to effective cancer control in China, India, and Russia. Lancet Oncol 2014;15:489–538.
[7] Bearz A, et al. Lung cancer in HIV positive patients: the GICAT experience. Eur Rev Med Pharmacol Sci 2014;18:500–8.
[8] Travis WD, et al. International association for the study of lung cancer/american thoracic society/european respiratory society international multidisciplinary classification of lung adenocarcinoma 2011;6:244–85.
[9] Dogan S, et al. Molecular epidemiology of EGFR and KRAS mutations in 3,026 lung adenocarcinomas: higher susceptibility of women to smoking-related KRAS-mutant cancers. Clin Canc Res 2012;18:6169–77.
[10] Kmietowicz. Use of e-cigarettes in UK has tripled in two years, finds survey 2014;348.
[11] Pendharkar D, et al. Molecular biology of lung cancer-a review. Indian J Surg Oncol 2013;4:120–4.
[12] Shi Y, et al. A prospective, molecular epidemiology study of EGFR mutations in Asian patients with advanced non-small-cell lung cancer of adenocarcinoma histology (PIONEER). J Thorac Oncol 2014;9:154–62.
[13] Baik IH, et al. Knockdown of RPL9 expression inhibits colorectal carcinoma growth via the inactivation of Id-1/NF-κB signaling axis. Int J Oncol 2016;49:1953–62.
[14] Zhang XL, et al. Serial analysis of gene expression in adenocarcinoma samples and normal colonic mucosa in a Chinese population. Genet Mol Res 2015;14:12903–11.
[15] Eid R, et al. Human ribosomal protein L9 is a Bax suppressor that promotes cell survival in yeast. FEMS Yeast Res 2014;14:495–507.
[16] Guo X, et al. Human ribosomal protein S13 promotes gastric cancer growth through down-regulating p27(Kip1). J Cell Mol Med 2011;15:296–306.
[17] Davis T. A characterisation of genes involved in apoptosis resistance. Stellenbosch: Stellenbosch University; 2013.
[18] Erdogan OS, et al. Genome-wide methylation profiles in monozygotic twins with discordance for ovarian carcinoma. Oncol Lett 2020;20:357.
[19] Ehrlich M. DNA hypomethylation in cancer cells. Epigenomics 2009;1:239–59.
[20] Franceschini A, et al. STRING v9.1: protein-protein interaction networks, with increased coverage and integration. Nucleic Acids Res 2013;41:D808–15.
[21] Dennis Jr G, et al. DAVID: database for annotation, visualization, and integrated discovery. Genome Biol 2003;4:P3.
[22] Waterhouse A, et al. SWISS-MODEL: homology modelling of protein structures and complexes. Nucleic Acids Res 2018;46:W296–w303.
[23] Kozakov D, et al. The ClusPro web server for protein-protein docking. Nat Protoc 2017;12:255–78.
[24] Pettersen EF, et al. UCSF Chimera–a visualization system for exploratory research and analysis. J Comput Chem 2004;25:1605–12.
[25] Mbita Z, et al. De-regulation of the RBBP6 isoform 3/DWNN in human cancers. Mol Cell Biochem 2012;362:249–62.
[26] Livak KJ, et al. Methods for qPCR gene expression profiling applied to 1440 lymphoblastoid single cells. Methods 2013;59:71–9.
[27] Sulima SO, et al. How ribosomes translate cancer, vol. 7; 2017. p. 1069–87.
[28] Bernard L, et al. Long-chain fatty acids differentially alter lipogenesis in bovine and caprine mammary slices. J Dairy Res 2013;80:89–95.
[29] Zhang X, et al. Structures and stabilization of kinetoplastid-specific split rRNAs revealed by comparing leishmanial and human ribosomes. Nat Commun 2016;7:13223.
[30] Kityk R, et al. Molecular mechanism of J-domain-triggered ATP hydrolysis by Hsp70 chaperones. Mol Cell 2018;69:227–37. e4.
[31] Bilder PW, et al. Crystal structure of the ancient, Fe-S scaffold IscA reveals a novel protein fold. Biochemistry 2004;43:133–9.
[32] Campeotto I, et al. Structural and mechanistic insight into the Listeria monocytogenes two-enzyme lipoteichoic acid synthesis system. J Biol Chem 2014;289:28054–69.
[33] Tina KG, et al. PIC: protein interactions calculator. Nucleic Acids Res 2007;35:W473–6.
[34] Iosefson O, Azem A. Reconstitution of the mitochondrial Hsp70 (mortalin)-p53 interaction using purified proteins–identification of additional interacting regions. FEBS Lett 2010;584:1080–4.
[35] Mayr JA, et al. Lipoic acid synthetase deficiency causes neonatal-onset epilepsy, defective mitochondrial energy metabolism, and glycine elevation. Am J Hum Genet 2011;89:792–7.
[36] Jain M, et al. Metabolite profiling identifies a key role for glycine in rapid cancer cell proliferation. Science 2012;336:1040–4.
[37] Tsurusaki Y, et al. Novel compound heterozygous LIAS mutations cause glycine encephalopathy. J Hum Genet 2015;60:631–5.
[38] Tort F, et al. Differential diagnosis of lipoic acid synthesis defects. J Inherit Metab Dis 2016;39:781–93.
[39] Hanahan D, Weinberg RA. Hallmarks of cancer: the next generation. Cell 2011;144:646–74.
[40] Stratton MR, et al. Canc Gen 2009;458:719–24.
[41] Hensley CT, et al. Glutamine and cancer: cell biology, physiology, and clinical opportunities. J Clin Invest 2013;123:3678–84.